

# Miscibility and Processibility in Linear Low Density Polyethylene and Ethylene–Propylene-Butene-1 Terpolymer Binary Blends

KYUCHEOL CHO,<sup>1</sup> TAE-KWANG AHN,<sup>2</sup> BYUNG H. LEE,<sup>1</sup> SOONJA CHOE<sup>2</sup>

<sup>1</sup>Taedok Institute of Technology, Yukong Ltd., Taejon, 305-370, Korea

<sup>2</sup>Department of Chemical Engineering, Inha University, Inchon, 402-751, Korea

Received 28 August 1995; accepted 30 May 1996

**ABSTRACT:** Blends of linear low density polyethylene (ethylene–octene-1 copolymer) and ethylene–propylene–butene-1 terpolymer (ter-PP) mixed in a twin-screw extruder have been characterized by using differential scanning calorimetry (DSC), dynamic mechanical thermal analysis, scanning electron microscopy (SEM), rheometric mechanical spectrometry, a capillary rheometer, and a universal test machine. Melting and crystallization behaviors by DSC and the  $\alpha$ ,  $\beta$ , and  $\gamma$  dynamic mechanical relaxations proposed that the blend is immiscible in the amorphous and crystalline phases by observing the characteristic peaks arised solely from those of the constituents. The lack of interfacial interaction between the components was suggested by the SEM study. A strong negative deviation of melt viscosity from the additive rule and the Cole–Cole plot confirmed the immiscibility in melt state. Incorporation of ter-PP induced a reduction in melt viscosity, shear stress, and final load. Flexural modulus and yield stress were linearly increased with ter-PP content, while the tensile strength and elongation at break were more or less changed. Although this blend system is immiscible in the solid and melt states, addition of less than 20 wt % ter-PP in the blend is viable for engineering applications with the advantages of improved processibility and mechanical properties. © 1997 John Wiley & Sons, Inc. *J Appl Polym Sci* **63:** 1265–1274, 1997

## INTRODUCTION

In general, mechanical properties of binary blends are unsatisfactory because the two components are immiscible or incompatible. One example is the case of the blend of polyethylene (PE) and polypropylene (PP). Despite the immiscibility, the PE/PP blend has been interesting, particularly in the industrial area, based on two terms<sup>1–3</sup>: the first aim is to improve physical or mechanical properties, including better processibility; and the second is to

solve recycling problems from an environmental point of view.

Among immiscible polyolefin blends, ethylene–propylene–diene terpolymer was used as a good compatibilizer.<sup>4,5</sup> In the linear low density polyethylene (LLDPE) (MI, 0.3)/PP (MI, 0.8) blends, small amounts of PP (under 5 wt %) induced miscible behavior by mechanical and rheological measurements.<sup>6,7</sup> Bartlett and colleagues<sup>8</sup> reported that PP (MI, 5.0)/high density PE (HDPE) (MI, 0.3) blends showed improved ductility only in the presence of a compatibilizer, such as an ethylene–propylene elastomer. The and coworkers<sup>9</sup> claimed that PP (MI, 20)/HDPE (MI, 13) at 90/10 ratio showed synergistic mechanical behavior due to

Correspondence to: S. Choe

© 1997 John Wiley & Sons, Inc. CCC 0021-8995/97/101265-10

the crystallization of which HDPE inhibits the nucleation rate and simultaneously minimizes the nucleation density of PP.

In the processing area of polyolefin, the molecular weight or molecular weight distribution (MWD) has an extensive affect on the rheological properties. In LLDPE/low density polyethylene (LDPE) blend systems, Muller and associates<sup>10</sup> reported that the melt viscosity of the blend upon shear stress was sensitive to the molecular weight of LDPE. In PP/HDPE and PP/LDPE systems which have similar molecular weights and MWDs, the melt viscosity under the same shear rate was observed in the order of HDPE > LDPE > PP. This was rationalized as a consequence of the difference in hydrodynamic volume in melt state.<sup>11</sup>

Mechanical properties of polyolefin blends have been another interest independent of miscibility. In the HDPE/LLDPE blend which was reported as a miscible system by the formation of the cocrystallization, the behavior of the flexural strength was explained by dividing in three sections, while the impact strength was increased with LLDPE content.<sup>12,13</sup> Moreover, there are several reports on polyolefin blends in the bases of miscibility, morphology, rheology, and optical and mechanical properties.<sup>14–17</sup>

The present paper investigates the role of ethylene-propylene-butene-1 terpolymer (ter-PP) as a minor component for improvements in processibility and modification of mechanical or rheological properties of the LLDPE/ter-PP blends. In addition, miscibility by thermal and morphological study are also discussed.

## EXPERIMENTAL

### Materials and Blends Preparation

The polymers used in this study were obtained from a commercial source and are listed in Table I. They are commercial grades with typical additives present. Seven LLDPE/ter-PP blends of varying compositions—100/0, 80/20, 60/40, 50/50, 40/60, 20/80, and 0/100 wt % (for differential scanning calorimetry [DSC] study, a few more blend compositions were made)—were prepared by a Brabender PL 2000 twin-screw extruder under barrel temperatures of 190, 200, and 210°C from the hopper to die and screw RPM of 50 using a counter-rotating screw. The extrudate from the die was quenched in water, pelletized, and then

dried. Sheet-type specimens for dynamic mechanical thermal analysis (DMTA), rheometric mechanical spectrometry (RMS), and a universal test machine were molded from the melt-blended pellet at 200°C using a hydraulic press (Wabash 30-1515), then cooled to 50°C on another hydraulic press.

### Instrumentation

Measurements of molecular weight of the homopolymers and blends were carried out using the Waters 150C GPC at 140°C and 1,2,4-trichlorobenzene as a solvent. A universal calibration curve obtained from standard polyethylene in the same solvent at 140°C was used for the molecular weight measurements of the unknown samples. The number and weight average molecular weights ( $M_n$  and  $M_w$ , respectively) of the LLDPE and ter-PP are listed in Table I. The  $M_n$  and  $M_w$  of the blends were linearly changed intermediate to those of the constituents. A similar trend was reported in the LLDPE/PP binary blends system.<sup>18</sup>

A Perkin-Elmer DSC-7 was used for the melting temperature ( $T_m$ ) and total enthalpy of fusion ( $\Delta H_f$ ), etc., under nitrogen atmosphere. Samples were first heated from 30 to 180°C at a heating rate of 10°C/min, annealed for 5 min at 180°C, cooled from 180 to 30°C at the cooling rate of 10°C/min, annealed at 30°C for 5 min, and rescanned from 30 to 180°C at the same heating rate. Then the  $T_m$  and  $\Delta H_f$  were obtained in the second scan, and crystallization temperature ( $T_c$ ) and total enthalpy of crystallization ( $\Delta H_c$ ) were obtained in the cooling process.

The  $\alpha$ ,  $\beta$ , and  $\gamma$  dynamic mechanical relaxations were observed by using the Polymer Laboratories DMTA MK-III in the range of -145–120°C under cryogenic conditions. Tensile mode at a constant frequency of 1 Hz and at a heating rate of 2°C/min was applied.

Morphological studies of the specimens were conducted using a Philips SEM-515 scanning electron microscopy (SEM) under an accelerated voltage of 20 kV and 5,000 magnitude. The samples were fractured in liquid nitrogen and coated with 300 Å gold in an Argon atmosphere.

For the rheological properties, a Rheometrics RMS-800/RDS-II and Instron capillary rheometer Model-3211 were used. For RMS, a circular plate-to-plate with a 2.5-cm diameter and continuous shear mode were applied at a frequency range of  $10^{-1}$  to  $10^2$  rad/s and at 190°C.  $\eta'$  (real

**Table I** Physical Properties of the Chemicals Used in This Study

Sample	Melt Index <sup>a</sup> (g/10 min)	Density <sup>a</sup> (g/cm <sup>3</sup> )	Monomer Content <sup>a</sup> (wt%)	$\bar{M}_w$ <sup>b</sup> (g/mole)	$\bar{M}_n$ <sup>b</sup> (g/mole)
LLDPE	0.91 at 190°C	0.919 at 23°C	1) ethylene 90.6 2) octene-1 9.4	93,000	31,000
ter-PP	0.91 at 230°C	0.89 at 23°C	1) ethylene 2.9 2) propylene 92.4 3) butene-1 4.7	131,000	42,300

<sup>a</sup> Data reported by supplier, Yukong Ltd.<sup>b</sup> Measured by GPC.

part of complex viscosity) and  $\eta''$  (imaginary part of complex viscosity) of the blends were measured for the Cole–Cole plot. The capillary rheometer was controlled at a shear rate of  $10^1$  to  $10^3$  s<sup>-1</sup> using a No. 1708 capillary with length/diameter of 5.0925/0.1275 cm (thus L/D = 40). The melt viscosity and shear stress were measured at 190°C.

The tensile properties were measured using an Instron Model 4301. The tensile specimens were dumbbell-shaped in 2.0 mm thickness, 12.6 mm width, and 25 mm gauge length. All the specimens were annealed at the constant temperature of 23°C and 50% humidity for at least 48 h before measurement. The tensile properties were collected using the ASTM D638-91a under a cross-head speed of 200 mm/min, and an ASTM D790-92 was used for flexural modulus at a compression speed of 1 mm/min.

## RESULTS AND DISCUSSION

### Thermal Analysis

The DSC thermograms of the melting and crystallization behaviors in LLDPE/ter-PP blend are shown in Figure 1. The LLDPE shows a narrow and sharp endothermic peak at 123°C, while ter-PP depicts two relatively broad and weak peaks at 135 and 153°C. For the blends, discrete melting peaks were observed representing the characteristics of the homopolymers. From this, LLDPE/ter-PP blends seem to be immiscible in the crystalline phase. The exothermic crystallization peak of LLDPE is sharp, which is similar to the melting behavior, and that of ter-PP is also sharp and large. Although the  $T_m$  of ter-PP is higher than that of LLDPE, the  $T_c$  of ter-PP as shown in Figure 1 is lower than that of LLDPE. The  $T_m$  and  $T_c$  of LLDPE are 123°C and 105°C, respectively, while those of homopolymer PP are 165°C and

92°C, respectively. Thus  $T_c$  of ter-PP would possibly be observed at a lower temperature, than that of LLDPE, which would arise from the different crystals between LLDPE and ter-PP.

The melting and crystallization temperatures from the DSC thermograms are depicted in Figure 2. As observed in Figure 1, two or three values of  $T_m$  or  $T_c$  were obtained, which indicates that LLDPE and ter-PP phases are separated in the whole range of blend compositions. An exception was observed at 90/10 but it is not certain because the endothermic peaks representing those of ter-PP were extremely weak even at 80/20. A 5% PP quantity in the PE/PP blend system was reported to miscible and the authors suggest that the blend system would be miscible upon blend ratio or mixing method, despite the thermodynamically immiscible system.<sup>6,13</sup> To analyze more in detail, the total  $\Delta H_f$  and  $\Delta H_c$  are displayed in Figure 3. Incorporation of ter-PP into LLDPE influenced a decrease in  $\Delta H_m$  and an increase in  $\Delta H_c$  (since the

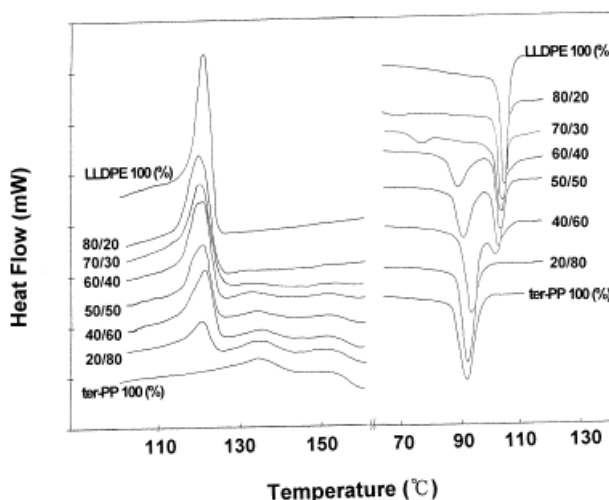


**Figure 1** DSC melting and crystallization thermograms in LLDPE/ter-PP blends.

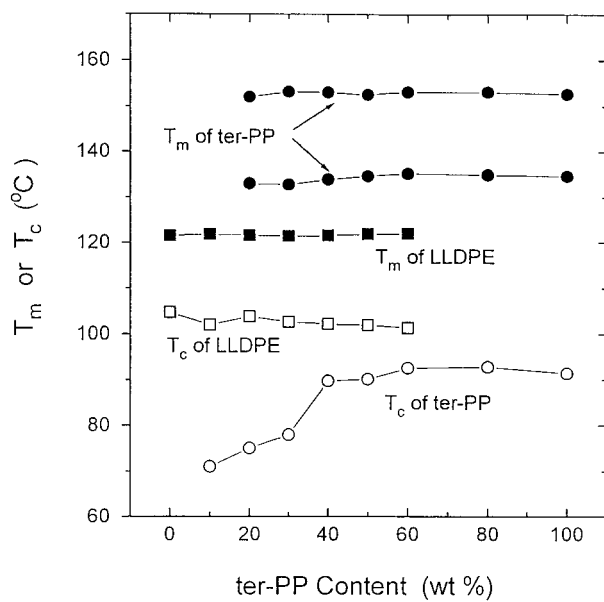


**Figure 2** Effect of blend compositions on melting and crystallization temperatures.

total enthalpy of crystallization is an exothermic process, it is plotted in the negative scale). Since  $\Delta H_m$  or  $T_m$  can be used as a reference of processing conditions, such as energy or the setting temperature of the extruder, a decrease in  $\Delta H_m$  may give an idea of improved processibility by mixing ter-PP into an LLDPE system.

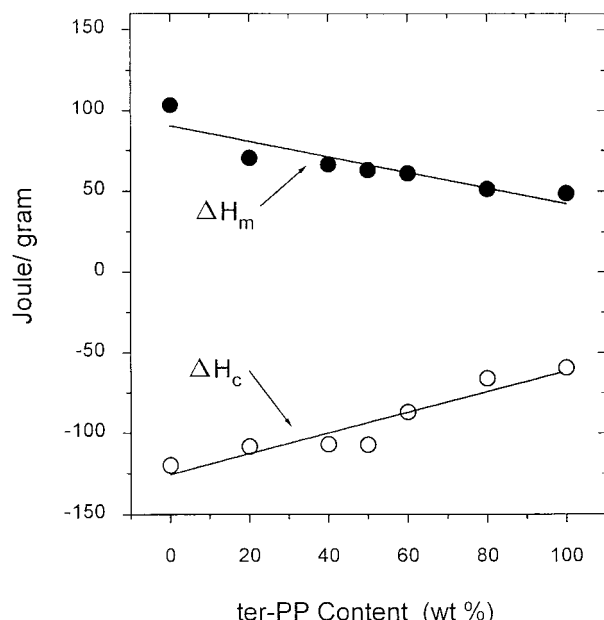


**Figure 3** Effect of blend compositions on the  $\Delta H_m$  and  $\Delta H_c$ .

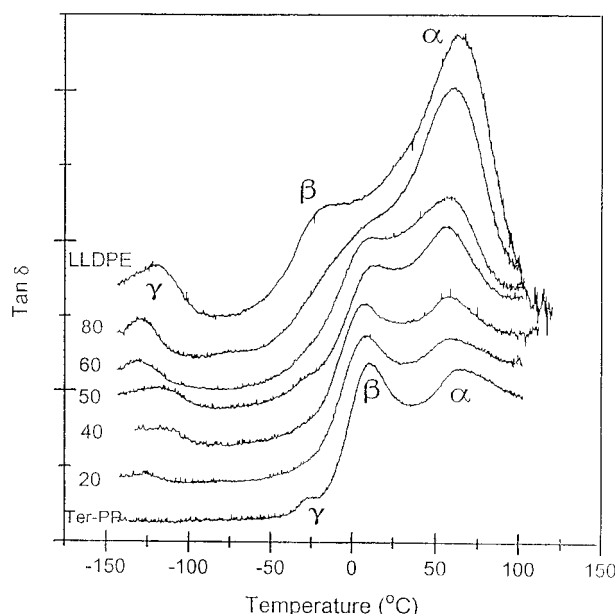


**Figure 4** Dynamic mechanical relaxations of the LLDPE/ter-PP blend in  $\tan \delta$ .

Damping  $\tan \delta$  obtained from the DMTA spectrum is shown in Figure 4 from  $-145$  to  $120^\circ\text{C}$ . In the order of higher temperature, the peaks are designated to the  $\alpha$ ,  $\beta$ , and  $\gamma$  relaxations or transitions. Sometimes the  $\alpha$  transition is specifically classified as  $\alpha$  and  $\alpha'$  transitions which may be affected by molecular scope motions.<sup>19</sup> LLDPE or ter-PP shows the  $\alpha$  relaxation only, compared to HDPE which has both the  $\alpha$  and  $\alpha'$ . The  $\alpha$  transition which is related to the melting behavior of the homopolymers and the blends was observed at almost the same position, but the peak intensity was decreased with ter-PP content. The intensity of the  $\alpha$  relaxation, which implies a crystal relaxation, is often discussed in terms of the lamellar thickness or long period of crystalline polymer. Takayanagi and Matsuo<sup>20</sup> observed that the long period and lamellar thickness of polyethylene single crystal mats was increased with respect to the annealing temperature, but that the intensity of the  $\alpha$  relaxation was decreased upon annealing temperature and increased with crystallization temperature. Sinnott<sup>21</sup> also reported that the peak intensity of the  $\alpha$  transition on annealing is inversely proportional to the lamellar thickness.

In general, the glass transition temperature ( $T_g$ ) of semicrystalline polymer is assigned to the  $\beta$  or  $\gamma$  transition, representing the amorphous fraction in semicrystalline phase or the side-chain effect. For example, there are disputes for accepting the  $\beta$  or  $\gamma$  relaxation of polyethylene as

the  $T_g$ .<sup>22</sup> We believe that the  $\beta$  relaxation of polyethylene is a representation of side-chain motion or a characteristic behavior of amorphous region.<sup>23</sup> The  $\beta$  transitions of LLDPE and ter-PP are shown at  $-20^\circ\text{C}$  and  $10^\circ\text{C}$ , respectively. Increasing the ter-PP content, the characteristic  $\beta$  peak position of each component was almost constant with change in intensity. From the observed  $\beta$  relaxation, the side chain of ter-PP behaves independently with no influence from that of LLDPE. The  $\gamma$  transition accepted as the  $T_g$  of LLDPE<sup>23</sup> and ter-PP in our laboratory was observed at  $-125^\circ\text{C}$  and  $-28^\circ\text{C}$ , respectively. Thus we may suggest that LLDPE is more flexible than ter-PP because the low temperature ( $\beta$  and  $\gamma$ ) relaxations of LLDPE are situated at lower temperatures than those of ter-PP. The  $\gamma$  transitions of the LLDPE/ter-PP blends occur at two different temperatures corresponding to that of LLDPE or ter-PP independent of ter-PP content. Since the  $\gamma$  relaxation is accepted as a characteristic of the amorphous phase and the  $\beta$  transition is explained by the side-chain effect, the above results which show separate  $\beta$  and  $\gamma$  relaxations may be interpreted as the side chains of the LLDPE/ter-PP blend behaving independently in the amorphous phase followed by formation of the immiscible system.

From the overall observation of the  $\alpha$ ,  $\beta$ , and  $\gamma$  relaxations, the LLDPE/ter-PP blend system is considered immiscible in both the amorphous and crystalline phases of the solid state.

### Morphology

The morphology of cryogenically fractured cross-sections of the specimen is displayed in Figure 5,(a) to (g). In Figure 5(b), the SEM micrograph of LLDPE/ter-PP 80/20 is differentiated from Figure 5(a) which represents homopolymer LLDPE. LLDPE is seen as the continuous phase, while ter-PP appears as holes removed during fracture. Adhesion between the spheres and continuous phase seems to be made. In the 60/40 blend [Fig. 5(c)], the size of ter-PP spheres seems to be unchanged, but coalescence of the ter-PP spheres is also observed. In particular, in the center of Figure 5(c), irregular (5–7  $\mu\text{m}$ ) ridges of coalescence connected to ter-PP were observed. However in Figure 5(d), the 50/50 composition, no more coalescence was observed. Instead, various sizes of spheres and holes (0.5–2  $\mu\text{m}$ ) representing the ter-PP were seen. The change in morphology between Figures 5(c) and 5(d) is dra-

matic, thus we believe that the phase inversion took place in the LLDPE/ter-PP 50/50 blend. In the 40/60 composition [Fig. 5(e)], ter-PP has turned to the continuous phase and the spheres and holes corresponding to LLDPE reduced to small size. In the 20/80 blend [Fig. 5(f)], the size of the spheres and holes is almost unchanged but the concentration of spheres has decreased. This is in good agreement with the report that in PE/PP blends, phase inversion occurred in 50/50 composition.<sup>1,2</sup> The morphological micrographs suggest that this binary system be phase-separated due to the weak interfacial force between two components.

### Rheological Properties and Processibility

In Figure 6, various shapes of  $\eta'$  versus  $\eta''$  of the blends are presented using a Cole–Cole plot. Cole–Cole plots are used to determine the miscibility or bimodality of amorphous or crystalline polymer blends; a good and smooth semicircular shape suggests a good miscibility or compatibility.<sup>18</sup> As seen in this figure, a well-defined semicircular shape was observed for the two homopolymers; whereas for the blends deviation from bimodality was observed, indicating that the melt flow of LLDPE/ter-PP blends is immiscible, representing that two phases exist in the melt state. But Dumoulin and colleagues<sup>24</sup> reported that the LLDPE (MI, 1.0)/PP (MI, 4.0) in 50/50 composition showed a partial compatibility in the presence or absence of compatibilizer. Although their system is similar to ours, the results are different. This may arise from the severe mixing conditions in their study from using a twin-screw extruder, W&P model ZSK 30. Utracki also reported that severe mixing may result in a different morphology.<sup>25</sup>

The dependence of the melt viscosity on the blend compositions at a fixed shear rate of 1160  $\text{s}^{-1}$  from the capillary rheometer is plotted in Figure 7. A strong, negative deviation from the log-additive rule was observed, indicating that this system is immiscible in the melt state. The miscibility of a blend is often characterized by using the above log-additive rule ( $\log \eta = \sum w_i / \log \eta_i$ )<sup>25</sup> or the Hayashida equation<sup>26</sup>:

$$1/\eta = w_i/\eta_i + w_j/\eta_j$$

where  $\eta$ ,  $\eta_i$  and  $\eta_j$  are the melt viscosity of the blend, polymer  $i$ , and polymer  $j$ , respectively, and

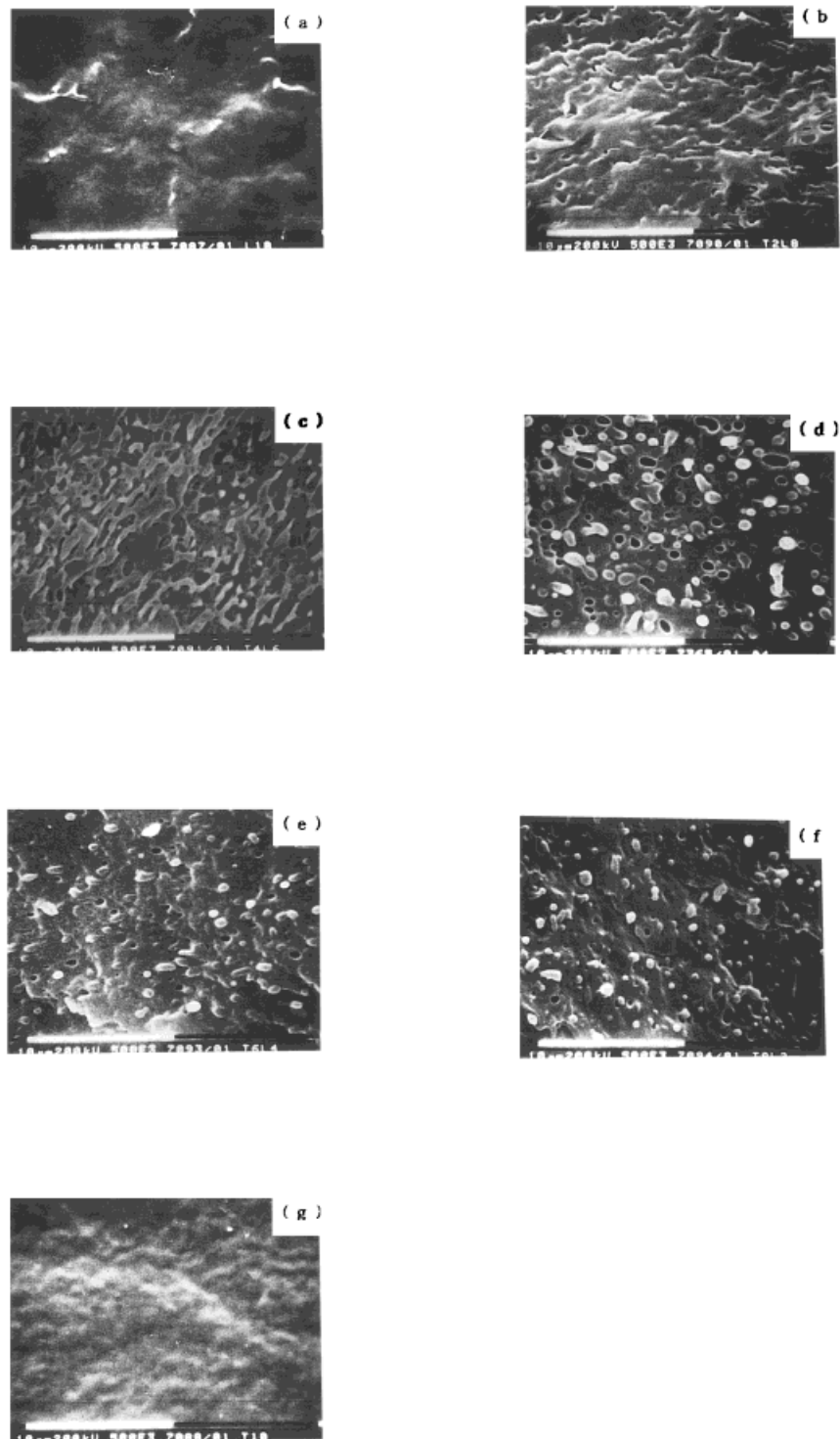


**Figure 5** Scanning electron micrographs of LLDPE/ter-PP blend ( $\times 5,000$ ): (a) LLDPE 100%; (b) LLDPE 80/ter-PP 20; (c) 60/40; (d) 50/50; (e) 40/60; (f) 20/80; (g) ter-PP 100%.

$w_i$  and  $w_j$  are the weight fractions of  $i$  and  $j$  components, respectively. The shear rate dependence of the melt viscosity and shear stress is shown in

Figure 8. All blends represent a typical non-Newtonian flow and a similar slope. In particular, the LLDPE/ter-PP 80/20 blend shows a dramatic de-

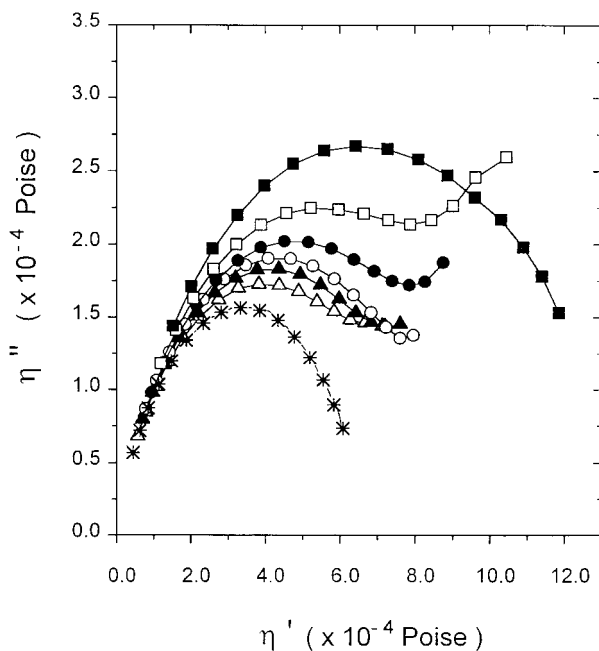


**Figure 6** Cole-Cole plot of LLDPE/ter-PP blend using  $\eta'$  and  $\eta''$ : ■, LLDPE 100%; □, LLDPE/ter-PP = 80/20; ●, 60/40; ○, 50/50; ▲, 40/60; △, 20/80; \*, ter-PP 100%.

crease in the melt viscosity and shear stress. This result suggests that an incorporation of 20 wt % of ter-PP give a better processing condition.

To analyze the role of ter-PP in the field, the

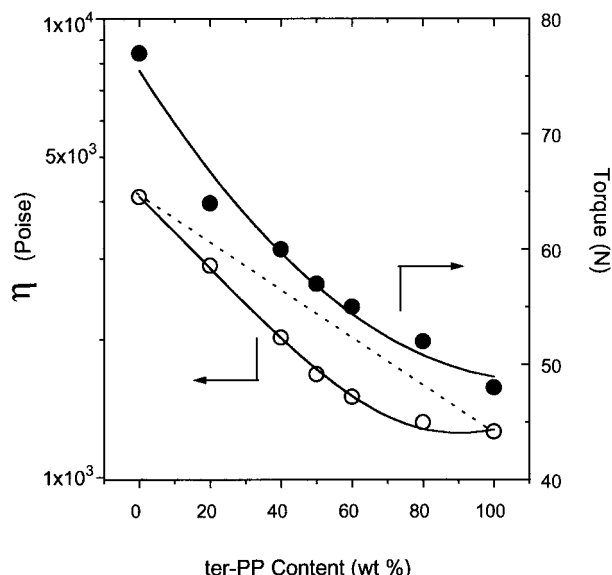


**Figure 7** Deviation from the additive rule of the melt viscosity versus ter-PP content, and dependence of the torque in LLDPE/ter-PP blend.

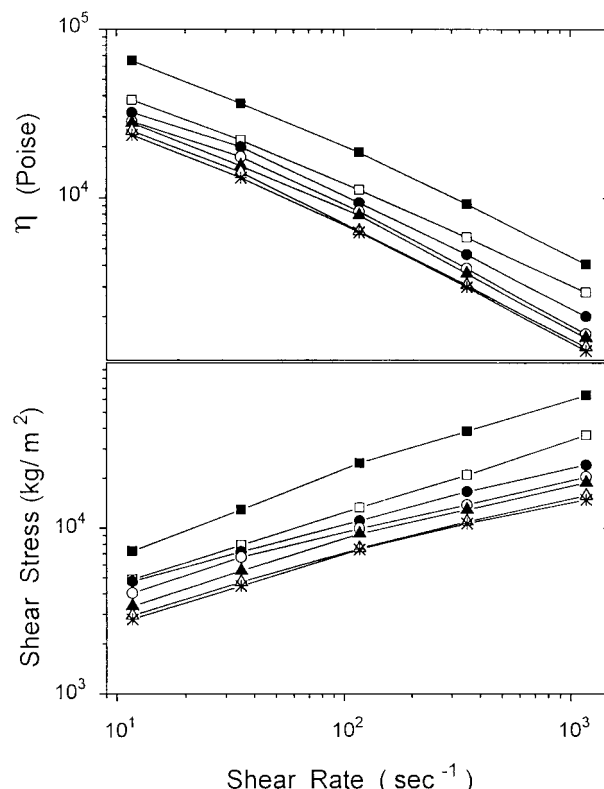


**Figure 8** Comparison of the viscosity and shear stress versus shear rate for LLDPE/ter-PP blend. The symbols are the same as in Figure 6.

final load of the blends was plotted in Figure 9 as a function of the shear rate. Since the final load can be converted as the extrusion load, it is an important factor in the field of manufacturing. Figure 9 implies that processability can be improved with addition of ter-PP. In particular, at the shear rate  $10^3 \text{ s}^{-1}$ , which is the practical shear rate in the field of extrusion, LLDPE/ter-PP 80/20 blend reduces the load from 650 kg to 400 kg, indicative of improved processing. Although ter-PP has higher molecular weight than LLDPE, the former shows lower melt viscosity or shear stress than the latter. It seems that ter-PP has many short side chains which may result in a short Gaussian coil, thus reducing hydrodynamic volume.<sup>27</sup> Figure 7 also displays the change of torque with changed ter-PP content, which is used for the actual evaluation of improvement in processability. At 80/20 (LLDPE/ter-PP) composition it drops dramatically, as predicted from capillary rheometer measurements. The above rheological investigations suggest that the blend system is immiscible in the melt state and that

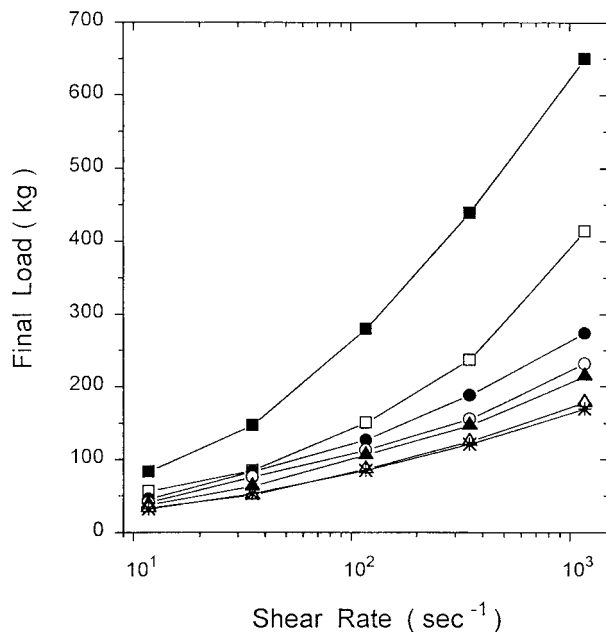


**Figure 9** Comparison of the final load versus shear rate for LLDPE/ter-PP blend. The symbols are the same as in Figure 6.

incorporation of small amounts (less than 20 wt %) of ter-PP in the blend improves the processibility and possibly economical production costs.

### Mechanical Properties

Load-strain curves for LLDPE/ter-PP blends are shown in Figure 10. Ductility was observed for

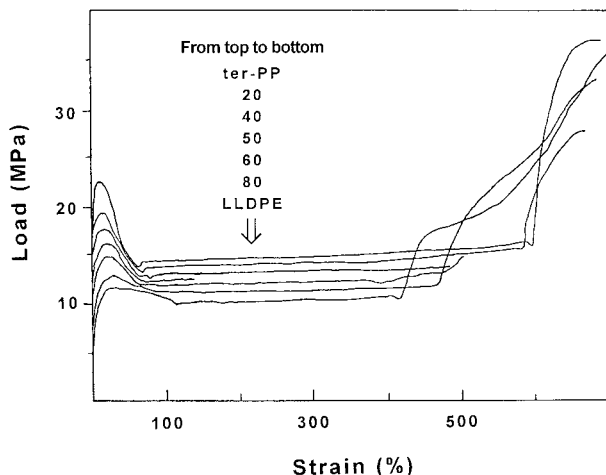


**Figure 10** Load-strain curves in LLDPE/ter-PP blend: Top to bottom LLDPE 100%; LLDPE/ter-PP = 80/20; LLDPE/ter-PP = 60/40; LLDPE/ter-PP = 50/50; LLDPE/ter-PP = 40/60; LLDPE/ter-PP = 20/80; ter-PP 100%.

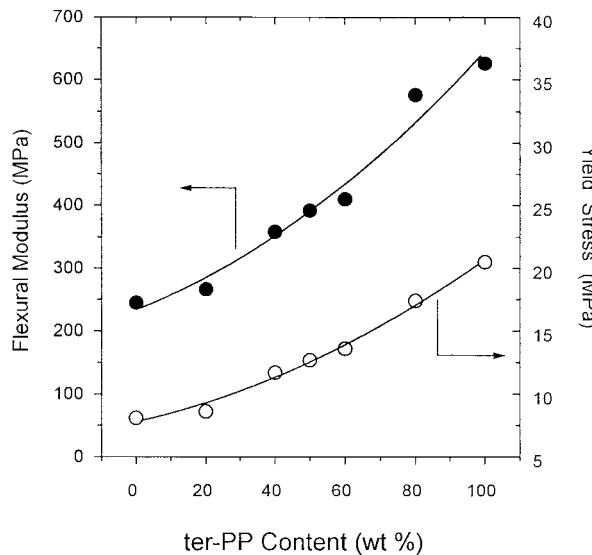


**Figure 11** Variation of tensile strength at yield in LLDPE/ter-PP blends: ○, yield stress; ●, flexural modulus.

the 80/20 and 20/80 LLDPE/ter-PP blends and the two homopolymers as well. Various tensile properties, such as yield stress, flexural modulus, tensile strength, and percent elongation at break, were calculated.

As seen in Figure 11, flexural modulus of the blends was linearly increased with ter-PP content, and yield stress as well. These are the same trend as the observed yield properties in the LLDPE/PP system.<sup>8,28</sup> Since yield property cannot be directly interpreted from the miscibility or compatibility, tensile strength and percent elongation at break of LLDPE/ter-PP blends were plotted in Figure 12. In this figure, the observed characteristics may be divided into three regions, depending on the blend compositions: (i) LLDPE-rich phase ( $\text{ter-PP} \leq 20 \text{ wt \%}$ ), (ii) the intermediate phase ( $30 < \text{ter-PP} < 70 \text{ wt \%}$ ), and (iii) ter-PP-rich phase ( $\text{ter-PP} \geq 80 \text{ wt \%}$ ). In the region of (i) or (iii), the tensile strength at break was slightly weakened, although the elongation at break was the same as the homopolymers. However in the region of (ii), the tensile strength and elongation at break dropped dramatically, which indicates the characteristics of an immiscible blend system by a discrete phase separation. Despite the immiscibility observed in the LLDPE/ter-PP blends, we believe that incorporation of 20 wt % ter-PP retains slightly improved mechanical properties.

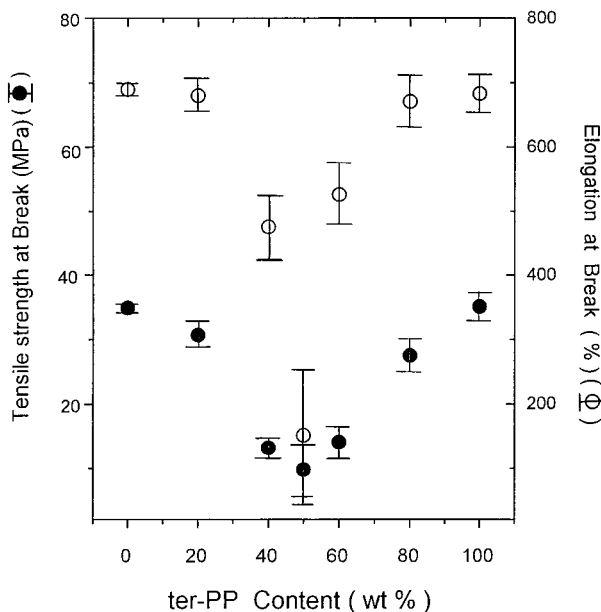


**Figure 12** Variation of tensile strength and elongation at break with error bars in LLDPE/ter-PP blends: ●, tensile strength at break; ○, elongation at break.

## CONCLUSIONS

We have studied the characteristics of LLDPE/ter-PP blends for the purpose of improved processability, economical production costs, and better mechanical properties. From DSC and DMTA measurements, two  $T_g$ 's were observed in whole-blend compositions. The  $\alpha$ ,  $\beta$ , and  $\gamma$  transitions observed from the dynamic mechanical relaxation showed that the characteristic peaks arise solely from those of the constituents. The above results suggest that LLDPE/ter-PP blends are immiscible in amorphous and crystalline phases in the solid state.

Morphological results were interpreted that this blend system is immiscible because of weak interfacial adhesion between the two components, and the phase inversion took place at 50/50 (LLDPE/ter-PP) composition.

The observed Cole–Cole plot, which deviated from the semicircular shape, and the dependence of the melt viscosity on the blend compositions supported the conclusion that this system is also immiscible in the melt state. Melt rheological properties showed that incorporation of ter-PP reduced the melt viscosity, shear stress,

and final load; thereby the processability could be improved.

In the region of LLDPE- or ter-PP-rich phases, mechanical properties in modulus and yield stress were improved and ductility was observed as well in the homopolymers. However the tensile strength at break was slightly weakened. Thus among the LLDPE/ter-PP blends, 80/20 composition may be used for engineering applications in terms of improved processability and production costs while retaining the improved yield behavior.

## REFERENCES

1. O. F. Noel and J. F. Carley, *Polym. Eng. Sci.*, **24**, 488 (1984).
2. M. J. Hill, *Polymer*, **35**, 3332 (1994).
3. V. Flaris, M. D. Zipper, G. P. Simon, and A. J. Hill, *Polym. Eng. Sci.*, **35**, 28 (1995).
4. R. E. Robertson and D. R. Paul, *J. Appl. Polym. Sci.*, **17**, 2579 (1973).
5. V. Choudhary, H. S. Varma, and I. K. Varma, *Polymer*, **32**, 2541 (1991).
6. M. M. Dumoulin and D. J. Carreau, *Polym. Eng. Sci.*, **27**, 1627 (1988).
7. W. N. Kim, S. I. Hong, J. S. Choi, and K. H. Lee, *J. Appl. Polym. Sci.*, **54**, 1741 (1994).
8. D. W. Bartlett, J. W. Barlow, and D. R. Paul, *J. Appl. Polym. Sci.*, **27**, 2351 (1982).
9. J. W. Teh, H. P. Blom, and A. Rudin, *Polymer*, **35**, 1680 (1994).
10. A. J. Muller, V. Balsamo, F. Da Silva, C. M. Rosales, and A. E. Saez, *Polym. Eng. Sci.*, **34**, 1455 (1994).
11. J. O. Lee, B. K. Kim, C. S. Ha, K. W. Song, J. K. Lee, and W. J. Cho, *Polymer (Korea)*, **18**, 68 (1994).
12. A. K. Gupta, S. K. Rana, and B. L. Deopura, *J. Appl. Polym. Sci.*, **44**, 719 (1992).
13. A. K. Gupta, S. K. Rana, and B. L. Deopura, *J. Appl. Polym. Sci.*, **49**, 477 (1993).
14. U. Plawky and W. Wenig, *J. Materials. Sci. Lett.*, **13**, 863 (1994).
15. R. G. Alamo, J. D. Londono, L. Mandelkern, F. C. Stehling, and G. D. Wignall, *Macromolecules*, **27**, 411 (1994).
16. G. D. Wignall, J. D. Londono, J. S. Lin, R. G. Alamo, M. J. Galante, and L. Mandelkern, *Macromolecules*, **28**, 3156 (1995).
17. J. N. Ness and J. Z. Liang, *J. Appl. Polym. Sci.*, **48**, 557 (1993).
18. L. A. Utracki, *Two Phase Polymer Systems*, L. A. Utracki, Ed., Hanser Publishers, Munich, 1991, p. 185.

19. M. Tagayanagi, in *Proc. Fourth Int. Cong. Rheol.*, Interscience Publishers, New York, 1965, p. 161.
20. M. Takayanagi and T. Matsuo, *J. Macromol. Sci.*, **B1**, 407 (1967).
21. K. M. Sinnot, *J. Appl. Phys.*, **37**, 3385 (1966).
22. N. G. McCrum, *Molecular Basis of Transition and Relaxations*, Dale J. Meier, Ed., Gorden and Breach Sci. Publisher, New York, 1978.
23. H. Lee, K. Cho, and S. Choe, *Macromolecules*, to appear.
24. M. M. Dumoulin, C. Farha, and L. A. Utracki, *Polym. Eng. Sci.*, **24**, 1319 (1984).
25. L. A. Utracki, *Am. Chem. Soc. Symp.*, 1989, Chap. 7, p. 153.
26. K. Hayashida, T. Takahashi, and M. Matsu, *Proc. Fifth Int. Cong. Rheol.*, Vol. 4, 1970, p. 525.
27. J. Rhee, Ph.D. Thesis, Northwestern University, Evanston, Illinois, 1992.
28. V. Flaris and Z. H. Stachurski, *J. Appl. Polym. Sci.*, **45**, 1789 (1992).